Bulletin of the Seismological Society of America, Vol. 99, No. 6, pp. 3510–3515, December 2009, doi: 10.1785/0120080366

Short Note

Coda-Wave Attenuation Imaging of Galeras Volcano, Colombia

by Jesús Lacruz,* Arantza Ugalde,† Carlos A. Vargas, and Eduard Carcolé‡

Abstract The spatial variation of *S*-wave coda attenuation (Q_c^{-1}) in the Galeras volcano region is analyzed. The study region is at present an active magmatic system situated in the southwestern Colombian Andes. Q_c^{-1} is estimated using seismograms from 435 volcano-tectonic earthquakes recorded at 31 stations of the Galeras seismograph network. Q_c^{-1} is then imaged using a 3D spatial stacking procedure. The technique is based on the assumption of uniform distribution of Q_c^{-1} over a spheroidal shell with its volume determined by the associated source–receiver distance. The resultant tomograms also show frequency dependence, which is interpreted in terms of the scale of the heterogeneities producing the scattering. High-attenuation anomalies are detected at high frequencies. Synthetic tests indicate the validity of the inversion technique.

Introduction

Galeras is a 4270 m high and 4500-year-old andesitic stratovolcano located in the southwestern Colombian Andes (Fig. 1). It is historically characterized by vulcanian-type explosions (Calvache, 1990). The most important one was recorded in 1936; it generated a pyroclastic flow to the northeast of the volcanic structure. The volcano lies 9 km from the city of Pasto; other towns are located on its flanks. In total, about 400,000 people live inside the hazard zone.

The complex tectonics of the region are the result of the collisions between the Nazca and South American plates that cause the uplift of the Andes and the volcanism in the region. The structural trend is N40°E and the main tectonic feature is the Romeral fault zone. This system includes the Silvia–Pijao and Buesaco faults, both of which cross under Galeras (Fig. 1).

Since 1988, when Galeras was reactivated after 50 yr of repose, it entered in a fumarolic and degassing stage, with seven eruptions between 1989 and 1993. An andesitic dome was extruded in September 1991, and it was destroyed during the July 1992 eruption. Since 1994, the volcano had been in a relatively calm stage with some ash and gas emission episodes and low-level eruptive activity until 2004, when a new eruptive episode began. Galeras continues to be active in 2009.

Seismicity in the region since 1988 has been characterized by long-period events, volcano-tectonic earthquakes, and tremor episodes (Gómez and Torres, 1997). The level of seismic activity has fluctuated, alternating between periods of low-level seismicity and episodes of increased seismic activity in terms of the number and/or magnitude of the events. Some shallow (up to 8 km) volcano-tectonic earthquakes have reached local magnitudes up to 4.7.

Since it was identified in 1990 as one of the decade volcanoes by the International Association of Volcanology and Chemistry of the Earth's Interior, Galeras has been extensively studied with the aim of achieving a better understanding of the volcano as well as assessing its seismic hazard. Many studies were devoted to the knowledge of the eruptive mechanism through geological, geochemical, and geophysical observations (e.g., Calvache and Williams, 1992; Stix *et al.*, 1993; Fischer *et al.*, 1994; Banks *et al.*, 1997; Calvache and Williams, 1997; Zapata *et al.*, 1997). In the seismological field, Narvaéz *et al.* (1997), Gómez *et al.* (1999), and Seidl *et al.* (1999) worked with the screw-type signals and the features of the different seismic sources. Coda Q, Q_c, was investigated by Gómez and Torres (1997) using low-frequency volcanic seismic events. Moncayo *et al.* (2004) studied temporal variations of Q_c at the volcano region. More recently, Carcolé *et al.* (2006) imaged the 3D spatial distribution of the relative scattering coefficients from shallow earthquakes that occurred under the volcano. They associated their findings of two strong scattering volumes, one located at shallow depths (between 4 and 8 km under the volcano summit) and one at a depth of ~37 km from the Earth's surface, with the magma chambers. This article attempts to tomographically image the Galeras

*Now at the CGGVeritas International, 49, Route de Meyrin, CP 252, 1211 Geneva 22, Switzerland, jesus.lacruz.ausin@cggveritas.com.

†Now at the Institut Geològic de Catalunya, Balmes, 209-211, 08006-Barcelona (Spain), augalde@igc.cat.

‡Now at Department of Geophysics, Graduate School of Science, Tohoku University, Aramaki-Aza-Aoba 6–3, Aoba-ku, Sendai-shi, Miyagi-ken, 980–8578, Japan, eduard@zisin.geophys.tohoku.ac.jp.

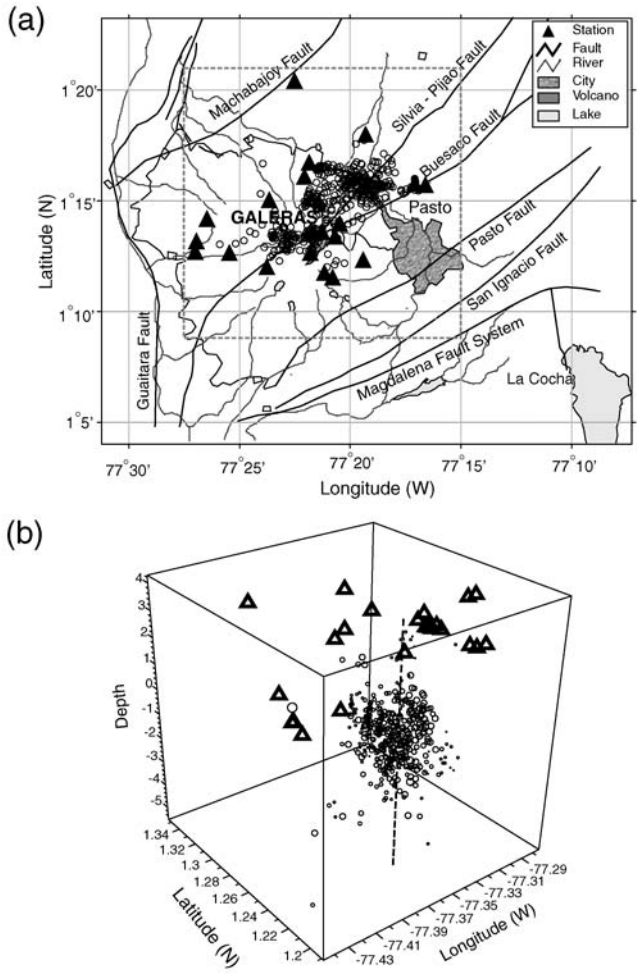

Figure 1. Map of the Galeras volcanic complex region showing the location of the epicenters and seismic stations used: (a) horizontal projection at the surface where the study area is indicated by a dotted square; and (b) a 3D representation of the stations and hypocenter locations.

volcano region using coda attenuation (Q_c^{-1}) measurements in 3D. Direct wave arrivals have been traditionally used to perform tomographic measurements; however, coda waves give more stable estimates because they are less sensitive to local path effects than direct waves as they sample a volume. A similar technique (in 2D) was successfully used by O'Doherty *et al.* (1997) for imaging the Long Valley caldera. The results of this article will serve to improve the knowledge about the internal structure of Galeras volcano.

Method

The decay rate of the coda amplitudes (Q_c^{-1}, coda attenuation) estimated within the framework of the single-scattering theory (Aki and Chouet, 1975) has proven useful for seismologists, because the simplicity of its measurement allows the study of its geographical and temporal variations relatively easily. Being an important subject in seismic risk analysis and engineering seismology, the knowledge of regional values of Q_c^{-1} and its spatial variation attracts considerable interest in relation to tectonics and seismicity studies (Singh and Herrmann, 1983; Jin and Aki, 1988). Coda waves are also useful for the deterministic characterization of the spatial heterogeneity in the lithosphere as an alternative to traditional tomographic measurements (O'Doherty *et al.*, 1997). Q_c^{-1} is a useful parameter for examining the interior of volcanoes because seismic attenuation is a physical parameter closely related to the thermal state of the volume sampled by the coda waves.

According to the single-scattering model (Aki and Chouet, 1975), Q_c^{-1} is estimated using the following equation:

$$P(\omega, t) = \frac{2g(\pi)|S(\omega)|^2}{\beta t^2} \exp\left(\frac{-\omega t}{Q_c}\right). \qquad (1)$$

In this expression, $P(\omega, t)$ is the time-dependent coda power spectrum, ω represents the angular frequency, β is the shear wave velocity, $|S(\omega)|$ is the source spectrum, and $g(\pi)$ is the directional scattering coefficient. The geometrical spreading is considered to be proportional to $1/r$, where r is the hypocentral distance; it only applies to body waves in a uniform medium. Because the source spectrum can be treated as a constant value for a single frequency, according to equation (1), Q_c^{-1} can be obtained as the slope of the least-squares fit of $\ln[t^2 P(\omega, t)]$ versus ωt, for $t > 2t_\beta$, where t_β is the S-wave travel time (Rautian and Khalturin, 1978).

According to Pulli (1984), seismic coda waves sample spheroidal volumes related to the source–receiver separation and the lapse time window considered. Therefore, Q_c^{-1} estimates from individual seismograms represent the average attenuation across the corresponding spheroidal volume. Multiple estimations of Q_c^{-1} for the same region from different source–receiver pairs allow repeated assessments of Q_c^{-1} with different sampling spheroids if we divide the region with a 3D grid made up of small cells. The corresponding Q_c^{-1} values from different spheroids in each cell can then be averaged to produce a Q_c^{-1} value for that cell. A version of this technique was first used by O'Doherty *et al.* (1997) for imaging the Long Valley caldera in eastern California.

Data Analysis and Results

Waveform data used in this article were selected from 435 well-located volcano-tectonic earthquakes over the period from 1989 through 2002 (Fig. 1). Coda magnitudes of these earthquakes were less than 2, with depths less than 6 km below the sea level, and hypocentral distances up to 16 km. A layered velocity structure adopted by the Observatorio Vulcanológico y Sismológico de Pasto (Table 1) was used for the locations (Moncayo *et al.*, 2004). A total of 31 short-period ($T_0 = 1$ sec), vertical-component recording stations used were located at distances less than 10 km from the active crater. The recorded ground motions were digitized at a rate of 100 samples per second, with the whole system having a flat velocity response between 1 and 25 Hz.

Table 1
Velocity Model* Used in Locating the Earthquakes†

Depth (km)	*S*-Wave Velocity (km/sec)
4	2.0
2	2.1
0	2.2
−4	3.4
−22	3.8
−40	4.5

*Based on personal communication with Diego Gómez, Observatorio Vulcanológico y Sismológico de Pasto, Colombia.
†The model is based on the work by Meissner *et al.* (1976).

Because different frequency bands contain information about scattering structures with different sizes comparable to the corresponding seismic wavelengths, and given that the signal energy decays abruptly for frequencies above 12 Hz, we decided to investigate the Q_c^{-1} behavior in frequency bands of 1–2 (1.5 ± 0.5) Hz, 2–4 (3 ± 1) Hz, 4–8 (6 ± 2) Hz, and 8–12 (10 ± 2) Hz.

From the band-pass-filtered seismograms, we calculated the time-dependent coda power spectrum $P(\omega, t)$ as the observed mean squared amplitudes $A_{\text{obs}}(\omega|r, t)$ for each hypocentral distance r. We used a time window of $2(r/\beta)$ to $2(r/\beta) + 10$ sec from the origin time of the earthquake for the calculation. The squared amplitudes were averaged in a 50% overlapping time window of $t \pm 2$ sec for the frequency band centered at 1.5 Hz, $t \pm 1$ sec for the frequency bands centered at 3 and 6 Hz, and $t \pm 0.5$ sec for the frequency band centered at 10 Hz. Then Q_c^{-1} was estimated for each seismogram by means of a least-squares regression of equation (1). Only those amplitudes that were higher than twice the background noise level were used for the regression, and only Q_c^{-1} values obtained from least-squares fits of equation (1) with correlation coefficients greater than 0.65 were kept.

Taking into account the distribution of stations and hypocenters, we chose a region of 22 km × 22 km in horizontal dimensions and 18 km in depth around the volcano for imaging. We then constructed the grid by dividing the region into $N = 100 \times 100 \times 18$ small cells. The grid used was selected, after several tests, by reaching an agreement between the accurate resolution and stability of the final tomogram, and the computing time required for performing the inversion. From the time window of the coda-wave the sampling spheroidal volumes in this case are confined in a shell, which is defined by $2(r/\beta) \leq TS + TR \leq 2(r/\beta) + 10$ sec, with $TS + TR$ being the lapse time required for the waves to travel from the source to any point of the grid (TS) and from there to the receiver (TR). All spheroidal shells were calculated by assuming the layered velocity structure shown in Table 1. To check for sampling insufficiencies, we computed the hit counts, or the number of Q_c^{-1} estimates contributed by the spheroids in each cell. We found that the entire region was sampled adequately although the number of hit counts was smaller inside a shallow area to the northeast of the

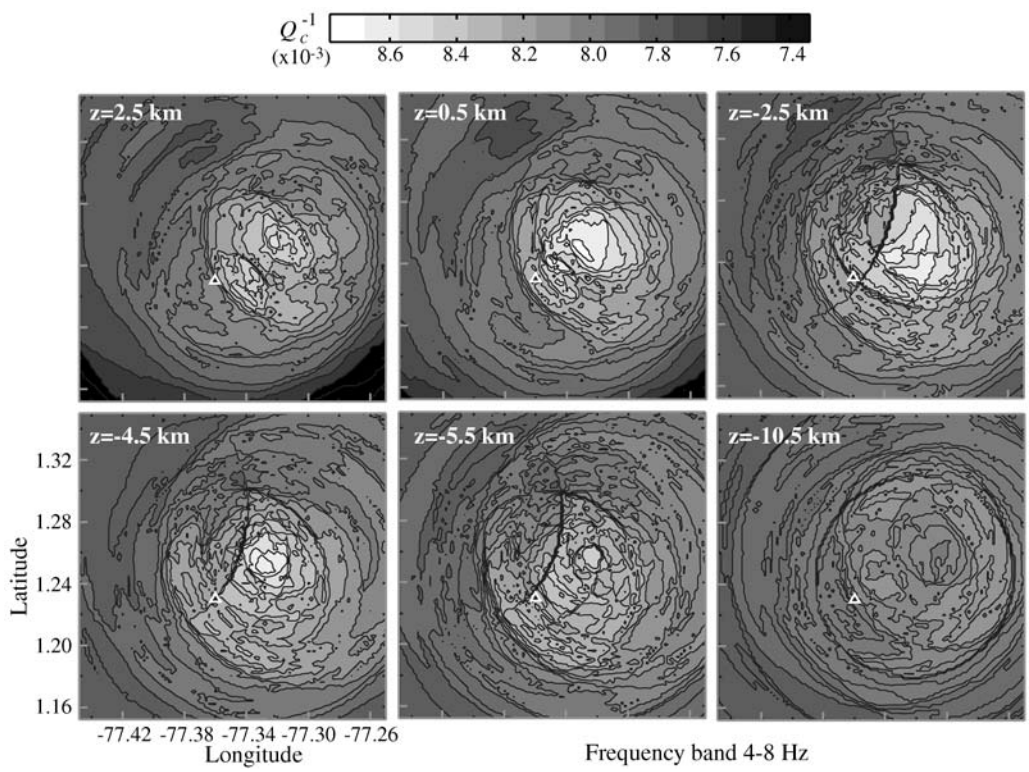

Figure 2. Horizontal sections of the study area showing the distribution of coda attenuation (Q_c^{-1}) at different depths indicated by z. The white solid triangle indicates the location of the Galeras volcano summit.

volcano summit. An example of the resultant tomogram showing the spatial distribution of coda attenuation in the study region for the 4–8 Hz frequency band and for different depths up to 15 km from the summit is plotted in Figure 2. The gray scale indicates the range of the Q_c^{-1} values. Zones of high and low coda attenuation are seen in the figure.

Figure 2 reveals a clear high-attenuation anomaly located to the northeast of the volcano summit. Vertical cross sections through 77.32° longitude and 1.24° latitude plotted in Figure 3 show the attenuation anomaly at depths between 2.5 km and −5 km. The Q_c^{-1} values show a 14% decrease from the center of the anomaly outward. For the 8–12 Hz frequency band, the same pattern is observed, but it is located slightly to the north of the vertical axis of the volcano and at depths between −1 km and −5 km. In this high-frequency range, the Q_c^{-1} values show a 46% decrease from the center of the anomaly outward. For the 1–2 and 2–4 Hz frequency bands, the tomograms present more uniform values of Q_c^{-1}, with values varying around 7% and 9%, respectively.

In order to assess the resolution and the validity of the results, we conducted a synthetic test. We simulated the presence of a high-attenuation structure with a volume of $6 \times 6 \times 6$ km^3 at the geographical location of the anomaly observed northeast of the volcano summit and at depths between 0 and −6 km from the Earth's surface. We did not change the locations of the sources and receivers and corresponding spheroidal shells. Average simulated Q_c^{-1} was assigned to the shells. In order to test if the results were an artifact of source and receiver locations, we put the high-attenuation structure slightly to the southwest of the volcano summit and repeated the procedure. Figure 4 shows the tomograms from the synthetic tests. It can be seen that the attenuation anomaly, including its change of location, is well-resolved. The difference in the shape of the anomaly might be affected by the source–receiver configuration. Comparing the synthetic tomograms of the two high-attenuation zones with different locations and comparing Figures 3 and 4, we conclude that, at shallow depths and high frequencies, a real high-attenuation structure located at the northeast of the volcano is resolved by the inversion.

Discussion and Conclusions

Carcolé *et al.* (2006) resolved relative scattering coefficient anomalies in a region that is spatially coincident with the high-attenuation pattern observed in this article. The current model of the magmatic plumbing system beneath Galeras volcano is based on petrologic and seismic data. It proposes a shallow conduit system with a distinct reservoir at a depth of 4–5 km from the summit, which is periodically fed from a deeper magma reservoir located at depths from kilometers to tens of kilometers (Calvache, 1990; Zapata *et al.*, 1997). The structure imaged in this article might be related to the shallow magmatic chamber of the Galeras plumbing system.

In conclusion, we used vertical-component seismograms from volcano-tectonic earthquakes to image the *S*-wave coda attenuation distribution in the Galeras volcano region. We employed a 3D spatial stacking technique using spheroids with uniformly distributed Q_c^{-1} values estimated from individual seismograms. A high-attenuation anomaly was found at shallow depths and high frequencies to the northeast of the volcano summit, which may be related to a possible area of magma accumulation.

Data and Resources

Seismic data used in this article are not accessible to the public. Activity reports of Galeras volcano are available at www.volcano.si.edu/ and www.ingeominas.gov.co/.

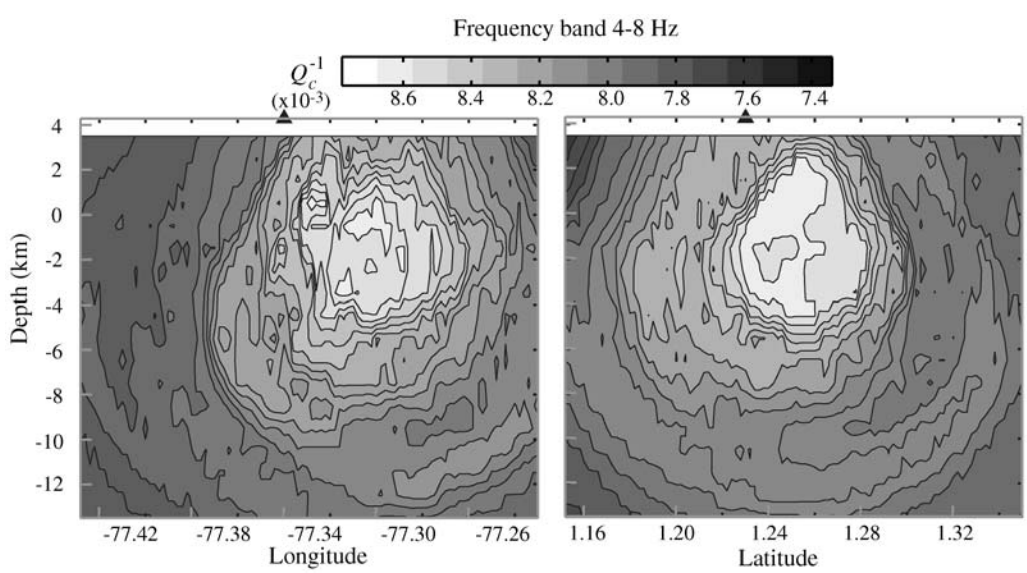

Figure 3. Vertical cross section of the study region along the two planes defined by the geographical coordinates: longitude −77.32° and latitude 1.24°. The solid triangle indicates the location of the Galeras volcano summit.

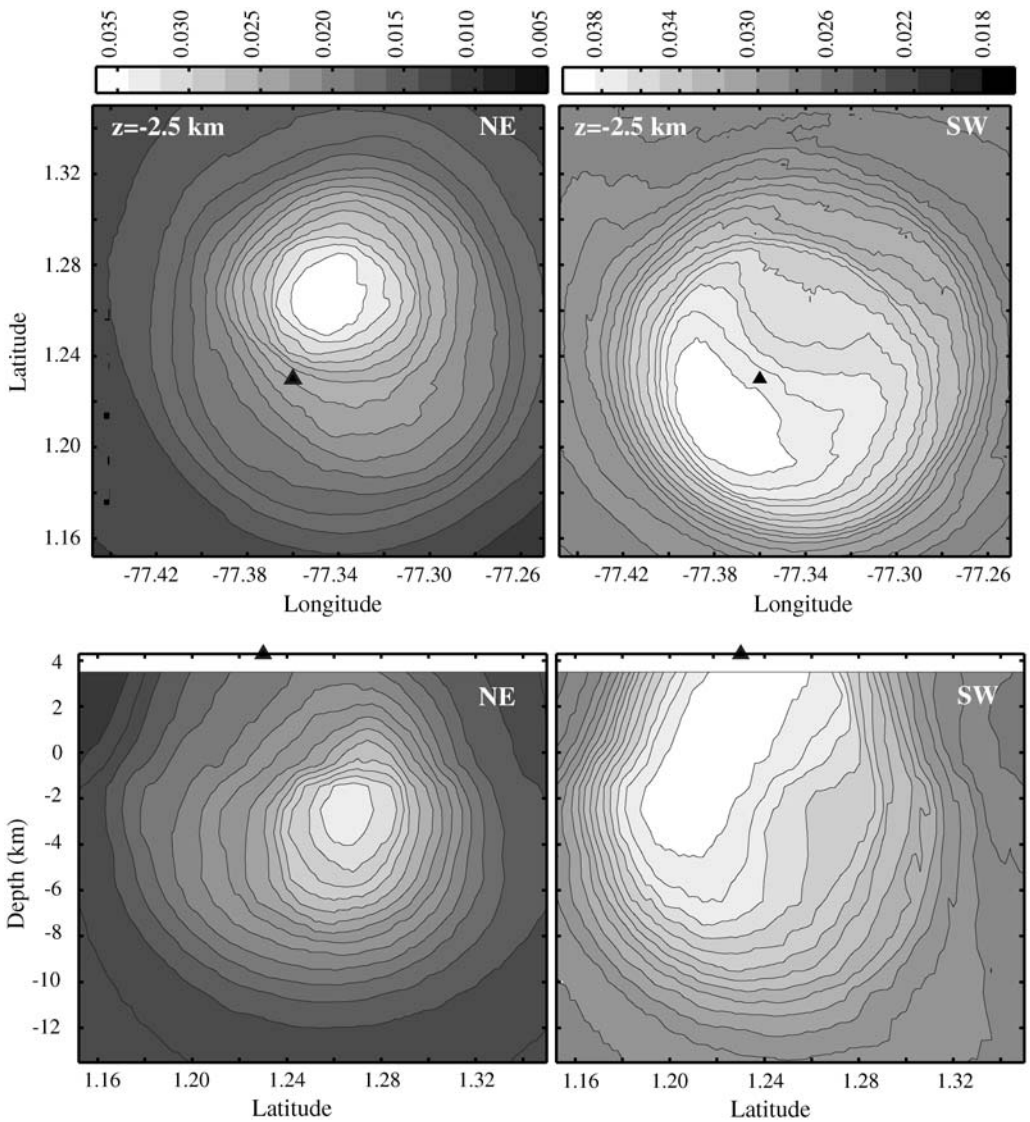

Figure 4. Horizontal sections (top) and vertical cross sections (bottom) of the tomograms associated with a synthetic test consisting of two close structures buried at depths between 0 and −6 km and located to the northeast (longitudes −77.38° to −77.32° W; latitudes 1.24° to 1.30° N) and southwest (longitudes −77.34° to −77.40° W; latitudes 1.16° to 1.22° N) of the volcano. The solid triangle indicates the location of the Galeras volcano summit.

Acknowledgments

We are very grateful to Diego Gómez and the people of the *Observatorio Vulcanológico y Sismológico de Pasto*, Colombia, for providing us with information about the recent activity history of the volcano and the seismic data used in this article. We also thank the associate editor, Charlotte A. Rowe, and an anonymous reviewer for comments that helped us to significantly improve this article.

E. Carcolé is enjoying a fellowship of the Global Center of Excellence program at Tohoku University, Sendai, Japan. This work started when he was contracted by a "Juan de la Cierva" program of the Spanish Ministerio de Ciencia y Tecnologia (MCYT). E. Carcolé acknowledges the support of the MCYT projects CGL-2005-04541-C03-02/BTE and CGL2008-00869/BTE.

References

Aki, K., and B. Chouet (1975). Origin of coda waves: Source, attenuation and scattering effects, *J. Geophys. Res.* **80,** 615–631.

Banks, N. G., M. L. Calvache, and S. N. Williams (1997). ^{14}C ages and activity for the past 50 ka at Volcán Galeras, Colombia, *J. Volcanol. Geotherm. Res.* **77,** 39–55.

Calvache, M. L. (1990). Geology and volcanology of the recent evolution of Galeras volcano, Colombia, *Master's Thesis*, Lousiana State University, Baton Rouge, Louisiana, 171 pp.

Calvache, M. L., and S. N. Williams (1992). Lithic-dominated pyroclastic flows at Galeras volcano, Colombia—An unrecognized volcanic hazard, *Geology* **20,** 539–542.

Calvache, M. L., and S. N. Williams (1997). Geochemistry and petrology of Galeras Volcanic Complex, Colombia, *J. Volcanol. Geotherm. Res.* **77,** 21–38.

Carcolé, E., A. Ugalde, and C. A. Vargas (2006). Three-dimensional spatial distribution of scatterers in Galeras volcano, Colombia, *Geophys. Res. Lett.* **33,** L08307, doi 10.1029/2006GL025751.

Fischer, T. P., M. Morrissey, M. L. Calvache, D. M. Gómez, R. A. Torres, J. Stix, and S. N. Williams (1994). Correlations between SO_2 flux and long-period seismicity at Galeras volcano, *Nature* **368,** 135–137.

Gómez, D. M., and R. A. Torres (1997). Unusual low-frequency volcanic seismic events with slowly decaying coda waves observed at Galeras and other volcanoes, *J. Volcanol. Geotherm. Res.* **77,** 173–193.

Gómez, D. M., R. A. Torres, D. Seidl, M. Hellweg, and H. Rademacher (1999). Tornillo seismic events at Galeras volcano, Colombia, a summary and new information from broadband three-component measurements, *Annali di Geofisica* **42,** 365–378.

Jin, A., and K. Aki (1988). Spatial and temporal correlation between coda *Q* and seismicity in China, *Bull. Seismol. Soc. Am.* **78,** 741–769.

Meissner, P. O., E. R. Flueh, F. Stribane, and E. Berg (1976). Dynamics of the active boundary in southwest Colombia according to recent geophysical measurements, *Tectonophysics* **35,** 113–136.

Moncayo, E. N., C. A. Vargas, and J. P. Durán (2004). Temporal variation of coda *Q* at Galeras volcano, Colombia, *Earth Sci. Res. J.* **8,** 19–24.

Narváez, L., R. A. Torres, D. M. Gómez, P. Cortés, H. Cepeda, and J. Stix (1997). "Tornillo"-type seismic signals at Galeras volcano, Colombia, 1992–1993, *J. Volcanol. Geotherm. Res.* **77,** 59–171.

O'Doherty, K. B., C. J. Bean, and J. Mc Closkey (1997). Coda wave imaging of the Long Valley caldera using a spatial stacking technique, *Geophys. Res. Lett.* **24,** 1545–1550.

Pulli, J. J. (1984). Attenuation of coda waves in New England, *Bull. Seismol. Soc. Am.* **74,** 1149–1166.

Rautian, T. J., and V. I. Khalturin (1978). The use of the coda for the determination of the earthquake source spectrum, *Bull. Seismol. Soc. Am.* **68,** 923–948.

Seidl, D., M. Hellweg, H. Rademacher, D. M. Gómez, and R. A. Torres (1999). The anatomy of a tornillo, puzzles from three-component measurements at Galeras volcano (Colombia), *Annali di Geofisica* **42,** 355–364.

Singh, S., and R. B. Herrmann (1983). Regionalization of crustal coda *Q* in the continental United States, *J. Geophys. Res.* **88,** 527–538.

Stix, J., J. Zapata, M. L. Calvache, G. Cortez, T. P. Fischer, D. Gómez, L. Narváez, M. Ordóñez, A. Ortega, R. A. Torres, and S. N. Williams (1993). A model of degassing at Galeras Volcano, Colombia, 1988–1993, *Geology* **21,** 963–967.

Zapata, J. A., M. L. Calvache, G. P. Cortés, T. P Fisher, G. Garzón, D. M. Gómez, L. Narváez, M. Ordóñez, A. Ortega, J. Stix, R. A. Torres, and S. N. Williams (1997). SO_2 fluxes from Galeras volcano, Colombia, 1989–1995, progressive degassing and conduit obstruction of a Decade volcano, *J. Volcanol. Geotherm. Res.* **77,** 195–208.

Observatori de l' Ebre
CSIC-URL
Horta Alta, 38
43520-Roquetes (Tarragona) Spain
jlajesus@gmail.com
augalde@obsebre.es
(J.L., A.U.)

Departamento de Geociencias
Universidad Nacional de Colombia
Bogotá, Colombia
cavargasj@unal.edu.co
(C.A.V.)

Universitat Politècnica de Catalunya
Departament d'Enginyeria del Terreny
Cartogràfica i Geofísica
Jordi Girona 1-3, Edifici 6 D2
08034 Barcelona, Spain
(E.C.)

Manuscript received 15 December 2008